Electron Cryomicroscopy of Acto-Myosin-S1 during Steady-State ATP Hydrolysis

M. Walker,* H. White,‡ B. Belknap,‡ and J. Trinick*

*AFRC Muscle and Collagen Research Group, Division of Molecular and Cell Biology, Department of Clinical Veterinary Science, Bristol University, Langford, Bristol BS18 7DY, United Kingdom; and ‡Biochemistry Department, Eastern Virginia Medical School, Norfolk, Virginia 23507 USA

ABSTRACT The structure of the complex of actin and myosin subfragment-1 (S1) during steady-state ATP hydrolysis has been examined by electron microscopy. This complex is normally dissociated by ATP in vitro but was stabilized here by low ionic strength. Optimal conditions for attachment were established by light-scattering experiments that showed that approximately 70% of S1 could be bound in the presence of ATP. Micrographs of the unstained complex in vitreous water suggest that S1 attaches to actin in a variety of configurations in ATP; this contrasts with the single attached configuration seen in the presence of ADP. The data are therefore compatible with the idea that a change in attached configuration of the myosin cross-bridge is the origin of muscle force. In control experiments where ATP was allowed to hydrolyze completely the binding of the S1 seemed cooperative.

INTRODUCTION

It is widely believed that muscle force derives from a gross structural change in the complex formed between the myosin head and actin. This change could be a variation in the attachment angle made with actin as first proposed by Huxley (1969); alternatively, it may be a conformational change within the head itself. These mechanisms have been collectively referred to as "tilting cross-bridge" models of force generation. Recent determination of the atomic structure of myosin subfragment-1 (S1) has led to a suggestion of how a large shape change within the head may occur (Rayment et al., 1993). However, although some form of tilting bridge remains the most likely origin of force, such a mechanism is still unproven.

The most direct way to search for large structural changes in cross-bridges is by electron microscopy. This has proven technically difficult because of the need to trap events happening on the millisecond scale while at the same time maintaining good preservation. Initial arrest of specimens has often been by freezing, because this is likely to be much faster than chemical fixation. Cooling rates in small specimens can be 10^6-10^7°C/s (Mayer and Astl, 1992), which results in water that is vitreous rather than crystalline. In the case of intact muscle rapidly frozen during contraction, acetone has usually been substituted for frozen water. This allows resin embedding and thin sectioning at ambient temperature (Tsukita and Yano, 1985; Craig et al., 1992; Hirose et al., 1993). However, although optical transforms from such sections resemble low angle x-ray transforms of muscle, a structure smaller than about 10 nm has been difficult to preserve, and the conformations of individual cross-bridges during contraction have not been described in detail.

Details as small as 2 nm can often be observed in solutions or suspensions of individual protein molecules or their assemblies, visualized by negative staining, metal shadowing, or frozen and unstained. In this way the structure of the strongly associated acto-S1 complex that occurs in ADP or in the absence of nucleotide has been defined to a resolution of ~3 nm and consists of S1 attached to actin filaments at roughly 45° (Moore et al., 1970; Milligan and Flicker, 1987). This angled S1 conformation is similar to the cross-bridge structure in rigor muscle and probably corresponds to the end of the cross-bridge power stroke. However, these electron microscope methods for solutions require protein concentrations that are approximately two orders of magnitude lower than the actin and myosin concentrations in muscle. They are therefore not directly applicable to weakly bound complexes that dissociate on dilution.

The energy for contraction comes from ATP hydrolysis, and this reaction is relatively well understood (reviewed in Hibberd and Trentham, 1986). The reaction is summarized in diagram 1.

$$\begin{array}{ccccccc} \text{AM} & \rightleftharpoons & \text{AM-ATP} & \rightleftharpoons & \text{AM-ADP-P} & \rightharpoonup & \text{AM-ADP} \rightharpoonup \text{AM} \\ & & \downuparrows & & \downuparrows & & \\ & & \text{M-ATP} & \rightleftharpoons & \text{M-ADP-P} & & \end{array} \quad (1)$$

The reaction intermediates can be divided into two classes, weakly bound and strongly bound. The binding of M-ATP and M-ADP-P to actin is 10^4-10^5 weaker than that of M or M-ADP, and it has been suggested that force is coupled to the weak-to-strong transition accompanying phosphate release (White and Taylor, 1976; Danzig et al., 1992). M-ATP and M-ADP-P consequently dissociate from actin at low protein concentration, which precludes direct study of their structure by the electron microscopy methods for solutions. A crucial test of tilting-bridge models of force production is

Received for publication 29 November 1993 and in final form 1 February 1994.

Address reprint requests to Dr. John Trinick, Dept. of Veterinary Medicine, Muscle/Collagen Research Group, University of Bristol, Bristol BS18 7DY, United Kingdom. Tel.: 44-934-852581(x9285); Fax: 44-934-852741; E-mail: j.trinick@bristol.ac.uk.

0006-3495/94/05/1563/10 $2.00

therefore whether these weakly bound states of the myosin head have a substantially different conformation from the ADP state.

One approach that prevents dissociation of acto-S1 by ATP is to covalently cross-link the complex (Stein et al., 1985). The cross-linked complex has a rate of ATP hydrolysis comparable to that of S1 at saturating actin. It was therefore argued that the primary effect of the cross-linking was to raise the local actin concentration to that required to stabilize the uncross-linked complex (i.e., similar to that in vivo). Electron micrographs of the covalent complex in ATP showed variable head attachment angles in both negatively stained (Craig et al., 1985) and frozen-hydrated specimens (Applegate and Flicker, 1987), which was taken to support a tilting mechanism of force production. Another possible explanation of these micrographs, however, is that the cross-link acted merely as a flexible tether.

An alternative way to stabilize weakly attached states of S1 is to lower the ionic strength (White and Taylor, 1976). Micrographs of acto-S1 in low salt during steady-state hydrolysis have recently been obtained, visualized by rotary shadowing after deep etching (Pollard et al., 1993). An important feature of these data was that the configuration of the attached S1 in ATP seemed similar to that in ADP or in the absence of nucleotide. This gave support to the view that micrographs of the cross-linked complex do not provide a realistic view of the cross-bridges going through the force-producing cycle; it also reinforced suggestions that nontilting mechanisms of cross-bridge action should be considered, based perhaps on bridges sliding along thin filaments without other gross changes in conformation (Vale and Oosawa, 1990). Conversely, Frado and Craig (1992) described the structure of acto-heavy meromyosin in ATP and reported differences from the ADP state. They briefly flushed (20–40 ms) the rigor complex with ATP before negative staining, after which disordered attachment was observed. In some cases the angle made by the heads with the filament was approximately 90°.

The different methods used to study the complex between actin and S1 (or heavy meromyosin) have therefore given contradictory results. In this paper we describe further electron microscopy of acto-S1-ATP stabilized by low ionic strength and visualized unstained in frozen-hydrated specimens. Association of the complex in ATP was explored by cosedimentation and light-scattering assays. Under optimal conditions ~70% of the S1 was attached to actin during steady state ATP hydrolysis. Micrographs of the complex under these conditions show a disordered pattern of labelling of the actin filaments by the S1. This suggests that S1 attaches in a variety of configurations in ATP. In some cases what we take to be individual S1 molecules can be observed in configurations different from the ADP state. The data are therefore compatible with a tilting mechanism of force generation. In control experiments in ADP a tendency toward cooperative binding was observed.

MATERIALS AND METHODS

Proteins

Rabbit skeletal muscle myosin and actin were prepared as previously described (White and Taylor, 1976). Two types of S1 were used: initial experiments were done with rabbit skeletal S1 containing the A1 light chain. This preparation is biochemically well characterized, and, at low ionic strength, the isozyme containing the A1 light chain binds with an affinity approximately 10-fold higher than the A2 isozyme (Chalovitch et al., 1984). The rabbit S1 was prepared from myosin with chymotrypsin, as previously described (Weeds and Taylor, 1975), except that 2 mg of lima bean trypsin inhibitor per mg of chymotrypsin rather than PMSF was used to inhibit chymotrypsin. The isozymes were separated by chromatography on a DEAE cellulose column equilibrated in 50 mM imidazole-HCl, pH 7.0 at 4°C, eluted with a gradient to 0.1 M KCl. Fractions were pooled to obtain S1 containing only the A1 light chain (A1-S1).

In later experiments cardiac S1 containing both LC1 and LC2 light chains was used. This was prepared by papain digestion of porcine cardiac myosin in the presence of Mg^{2+} according to a method provided by R. Smith and I. Rayment (personal communication). The cardiac S1 binds to actin as strongly as the A1 fraction of rabbit skeletal S1 (data not shown) and is a single isozyme. Cardiac S1 should be more easily visualized by electron microscopy than the skeletal S1, because retention of the LC2 light chain should give a longer molecule (Vibert and Craig, 1982; Flicker et al., 1983; Walker and Trinick, 1989). The rates of several of the first order steps of the ATPase mechanism are also considerably slower for cardiac S1 than fast skeletal S1, which allows more time before ATP exhaustion. The amount of S1 bound to actin during steady-state hydrolysis was determined from the 350-nm light scattered at 90° using a Perkin-Elmer (Norwalk, CT) 3000 fluorescence spectrometer operating at 20°C with a thermostatted cuvette.

Electron microscopy

Vitrified aqueous specimens for electron microscopy were prepared by plunge freezing into condensed ethane (Adrian et al., 1984; Trinick et al., 1986). Before mixing, actin and S1 were dialyzed at a concentration of roughly 10 mg/ml into 5 mM 3-[N-morpholino]propane-sulphonic acid (MOPS), 2 mM $MgCl_2$, 1 mM dithiothreitol (DTT), pH 7.0 at 0°C. Mixing was performed in 2 stages: the S1 and actin were first combined and diluted with dialysate to 5 × the required final concentration in a volume of 40 μl. After gentle mixing for 5 min this solution was diluted with 160 μl of a solution containing 0.25 mM ATP, pH 7.0, in water, so that the final ionic strength was ~2 mM. Ten microliters of the final mixture was immediately applied to a holey-carbon-coated grid, which had previously been glow discharged in an amylamine atmosphere, and the grid was blotted with filter paper and frozen. The interval between addition of the ATP and freezing was approximately 15 s. ATPase assays showed that, under the conditions used, hydrolysis would not be complete in less than 1 min. In control experiments ATP was omitted, and water was used to make the final dilution. Alternatively, the reaction was allowed to incubate for 5–10 min after addition of the ATP so as to allow complete hydrolysis. The filter paper used to blot the grids was Whatman (Maidstone, Kent, UK) Grade 52, because tests showed that in specimens blotted with the more usual Grade 1 paper significant amounts of calcium can accumulate (Berriman and Trinick, unpublished data). The freezing apparatus used held the grid in a wet filter paper sandwich until just before (~5 ms) entry into the ethane; this reduces concentration of solutes that can occur through evaporation from the thinned aqueous layer (Trinick and Cooper, 1990). The vitrified specimens were stored in liquid nitrogen or transferred directly to the loading station of a Gatan (Pleasanton, CA) model 626 cold specimen holder. To minimize condensation of water onto the specimen inside the microscope, the sliding frost shield on the holder was not opened until the partial pressure of water fell to $<5.10^{-8}$ torr (measured by residual gas analyzer). The holder was operated at ~−170°C in a Jeol (Tokyo, Japan) 1200ex microscope fitted with SHP10 pole-pieces and a modified double blade anticontaminator held at −182°C. Low dose micrographs (~10 e/Å^2) were exposed at 40,000 ×

magnification after defocusing by ~2 μm at 80,000 × magnification and processed for 12 min in full strength D19 developer.

RESULTS

Association of the acto-S1 complex in ATP

To maximize binding of S1 to actin during ATP hydrolysis, conditions were explored to allow the minimum ionic strength compatible with protein stability and pH buffering requirements. Fig. 1 shows the changes in light scattering observed during the hydrolysis of ATP under the conditions used in the electron microscopy (1 mM MOPS, 0.2 mM $MgCl_2$, 0.2 mM MgATP, pH 7, 4°C). After establishing the baseline, 0.1 ml of 2 mM MgATP was added to 0.9 ml of solution containing 5 μM actin and 4 μM S1 in 1 mM MOPS, 0.4 mM $MgCl_2$, pH 7. After mixing, the light scattering decreased approximately 30% from the level measured with acto-S1 compared with that measured for actin alone. The scattering remained constant for ~1 min before returning to a level slightly less than that obtained before the addition of ATP. When ATP was added to a similar solution that also contained 100 mM KCl, the light scattering decreased to a level indistinguishable from that for actin alone. These data indicate that under the conditions used approximately 70% of the S1 is bound to actin at low ionic strength during steady-state hydrolysis. This is consistent with an apparent binding constant of approximately 2 μM.

Tests were also made of the stability of the proteins and the adequacy of the pH buffering under the conditions used.

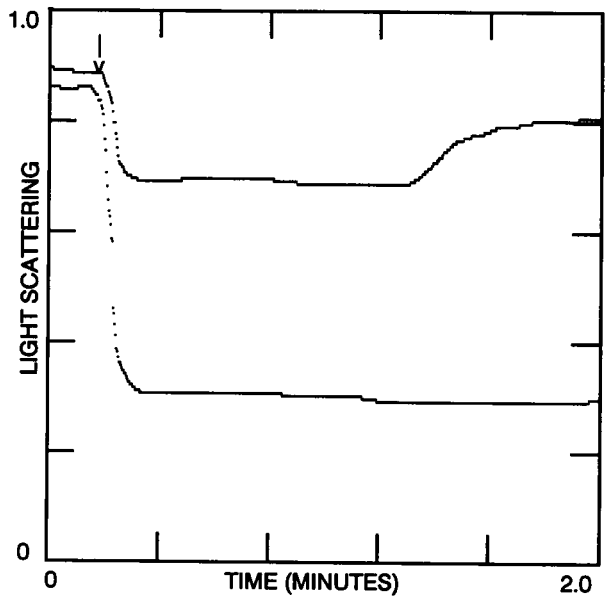

FIGURE 1 Light-scattering measurements of S1 binding to actin during steady-state ATP hydrolysis. The top trace shows the 350-nm light scattered at 90° from a solution containing 5 μM actin and 4 μM S1-A1. ATP was added to give a final concentration of 200 μM at the time indicated by the arrow in the upper left corner of the figure. A similar experiment in which the solution also contained 100 mM KCl is shown by the lower trace.

In 1 mM MOPS, 0.4 mM $MgCl_2$, 0.2 mM ATP, pH 7, A1-S1 loses approximately 20% of its enzymatic activity per day, and aggregation of the actin filaments can be observed after 24 h. However, in the 5 mM MOPS buffer the actin and S1 were stable for ~1 week, as judged by ATPase assays and electron microscopy. Actin and S1 in very low ionic strength buffer were therefore obtained by first dialyzing against 5 mM MOPS, 2 mM $MgCl_2$, pH 7, followed by fivefold dilution with ice-cold distilled water immediately before use. After complete hydrolysis of 0.2 mM ATP the pH had decreased only slightly from 7.0 to 6.8.

Electron microscopy of acto-S1-ATP

Fig. 2 shows a micrograph of a mixture of rabbit skeletal A1-S1 and actin frozen during steady-state ATP hydrolysis at low ionic strength. The concentrations used in this specimen were 5 μM actin and 4 μM S1 and were the same as used for the light-scattering measurements described above. These concentrations are close to the maximum practical for the electron microscope specimens. In the background of the micrograph there are many small particles that generally appear as small spots (~10 nm in diameter) but are sometimes elongated. These particles were not present in control experiments with no S1, and we therefore take them to be individual S1 molecules. Comparison of the filaments in Fig. 2 with actin filaments in the absence of S1 (see unlabeled actin in Trinick et al., 1986; also in Fig. 5 below) shows that there was clearly extensive binding of the S1 to the actin. Binding of S1 to the actin in Fig. 2 is best observed by sighting along the filaments from the edge of the micrograph. Fig. 2 therefore confirms that it is possible to use low ionic strength to bind a substantial fraction of S1 to actin during steady-state ATP hydrolysis. The exact extent of labelling of the actin is difficult to estimate from micrographs, but the overall appearance is compatible with the estimate from light scattering that ~70% of the S1 is bound. The maximum width of the labelled filaments was approximately 30 nm.

The pattern of S1 labelling of actin filaments in Fig. 2 is irregular, and the filaments have a disordered structure. This disorder seems to result from S1 being attached to the filaments in a variety of conformations, as opposed to groups of S1 molecules bound in one configuration with gaps in between. These filaments have a very different appearance from the characteristic "arrowhead" structure of filaments labelled in the presence of ADP or no nucleotide (see below).

The filaments in Fig. 2 were relatively heavily labelled to demonstrate unequivocally that a substantial fraction of S1 can be bound to actin in the presence of ATP. However, at this high degree of labelling many of the S1 molecules are close together or superimposed, which makes it difficult to discern individual attachment conformations. To see more detail, the protein concentrations were lowered to give sparser labelling, and we used S1 from porcine cardiac muscle. The cardiac S1 retains both light chains and is therefore likely to be a longer molecule (see Vibert and Craig,

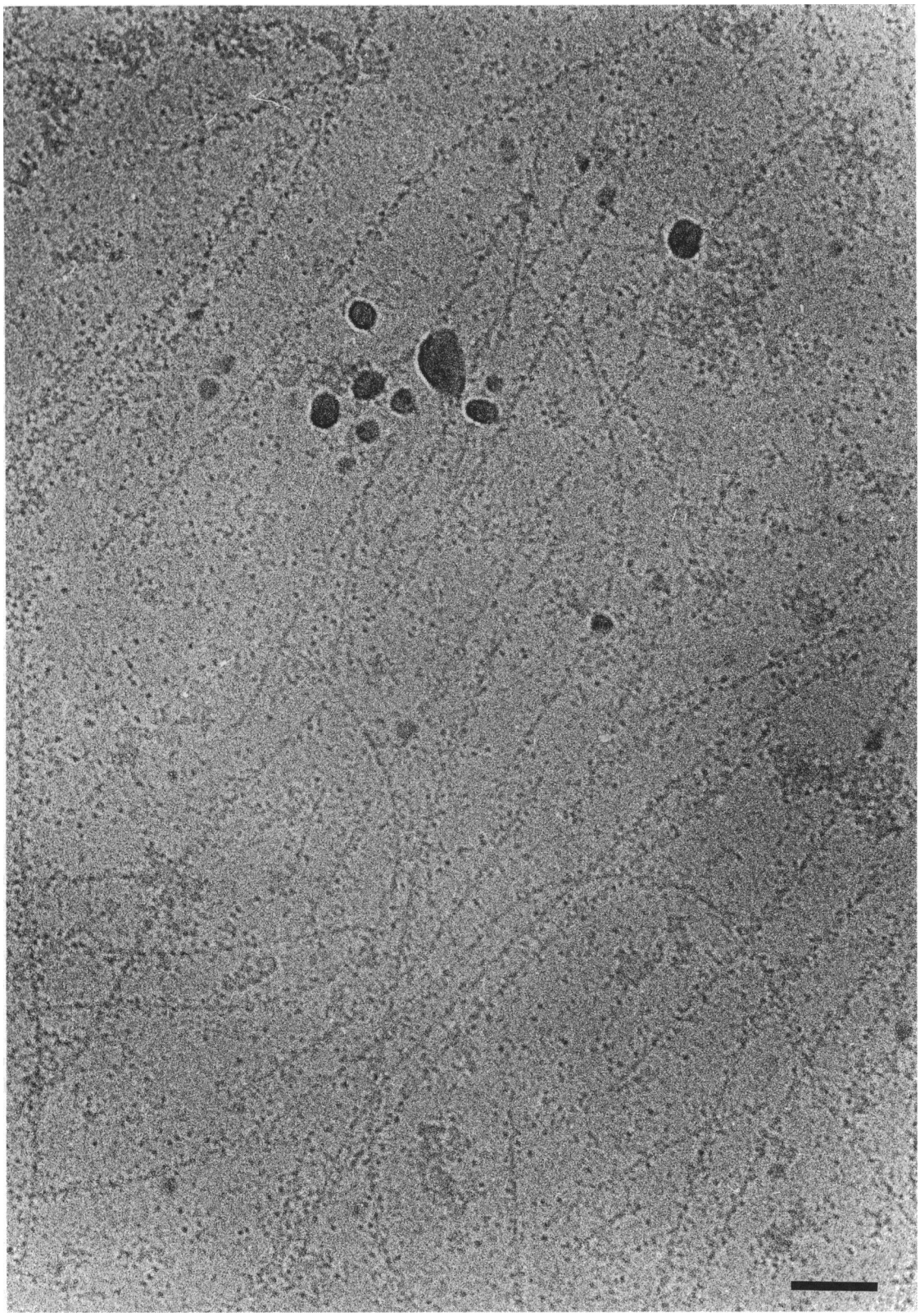

FIGURE 2 Actin (5 μM) decorated with rabbit skeletal muscle S1-A1 (4 μM) frozen in steady-state ATP hydrolysis. The scale bar shows 100 nm.

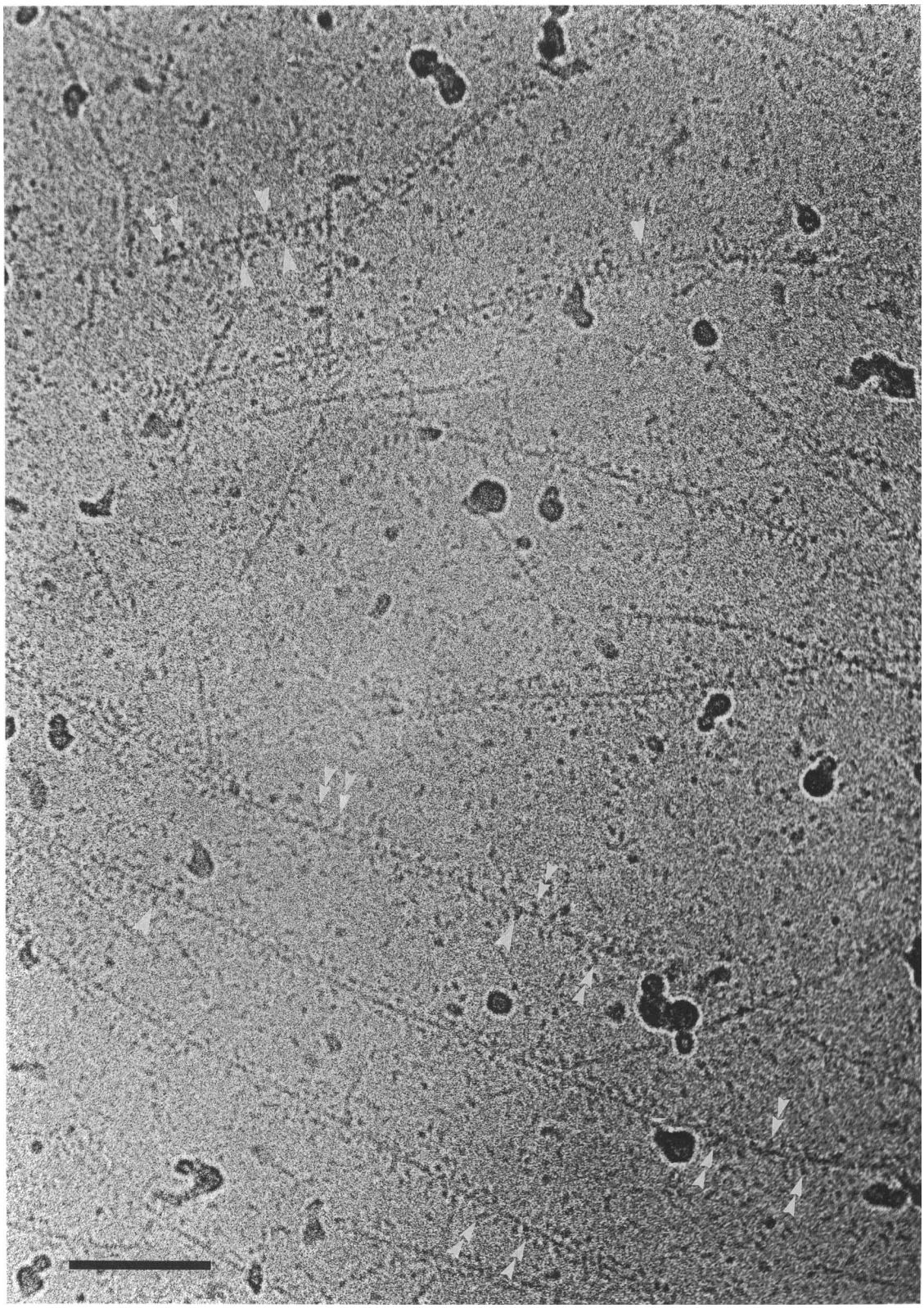

FIGURE 3 Actin (4 μM) decorated with porcine cardiac muscle S1 (2.3 μM) in steady-state ATP hydrolysis. Single arrows point to areas where what are presumably individual S1 molecules are clearly visible. Double arrows show where the angle between the long axis of the S1 and the filament long axis can be in different quadrants (i.e., <90° and >90°) on the same filament. The scale bar shows 100 nm.

1982; Flicker et al., 1983; Walker and Trinick, 1989). Fig. 3 shows a micrograph of actin labelled with cardiac S1 in ATP. In a number of cases individual S1 molecules can be seen attached to the actin, and these have a more elongated appearance than those in Fig 2. In some cases the attached S1 also appears curved. The maximum length and width of the S1 were about 17 and 7 nm, respectively. The maximum width of the labelled filaments was approximately 35 nm, which is also consistent with the cardiac S1 being longer than the skeletal muscle molecule. In some cases the angle of attachment defined by the long axis of the S1 is roughly at right angles to the long axis of the actin filament. Cases were also visible in which the angle made by different S1 molecules on the same filament are in different quadrants (i.e., <90° or >90°).

Fig. 4 shows a montage of actin filaments decorated in the presence of ATP with porcine cardiac S1. The data are similar to that in Fig. 3, in that individual S1 configurations can sometimes be discerned. A feature of both Figs. 3 and 4 is that, although individual S1 conformations are usually difficult to describe with certainty, the bulk of the S1 seems to be located ~10 nm from the edge of the actin. Thus, when viewing the micrograph from its edges and sighting along a filament there can often be seen a reduction in the density of material close to the filament and then an increase in density at a distance of roughly 10 nm from the edge of the actin.

ADP state

Fig. 5 shows a micrograph of a specimen prepared in a similar way to Figs. 2, 3 and 4, except that after addition of the ATP the mixture was allowed to incubate for 5 min at room temperature. Most of the filaments have the characteristic appearance, termed arrowhead, caused by regular attachment

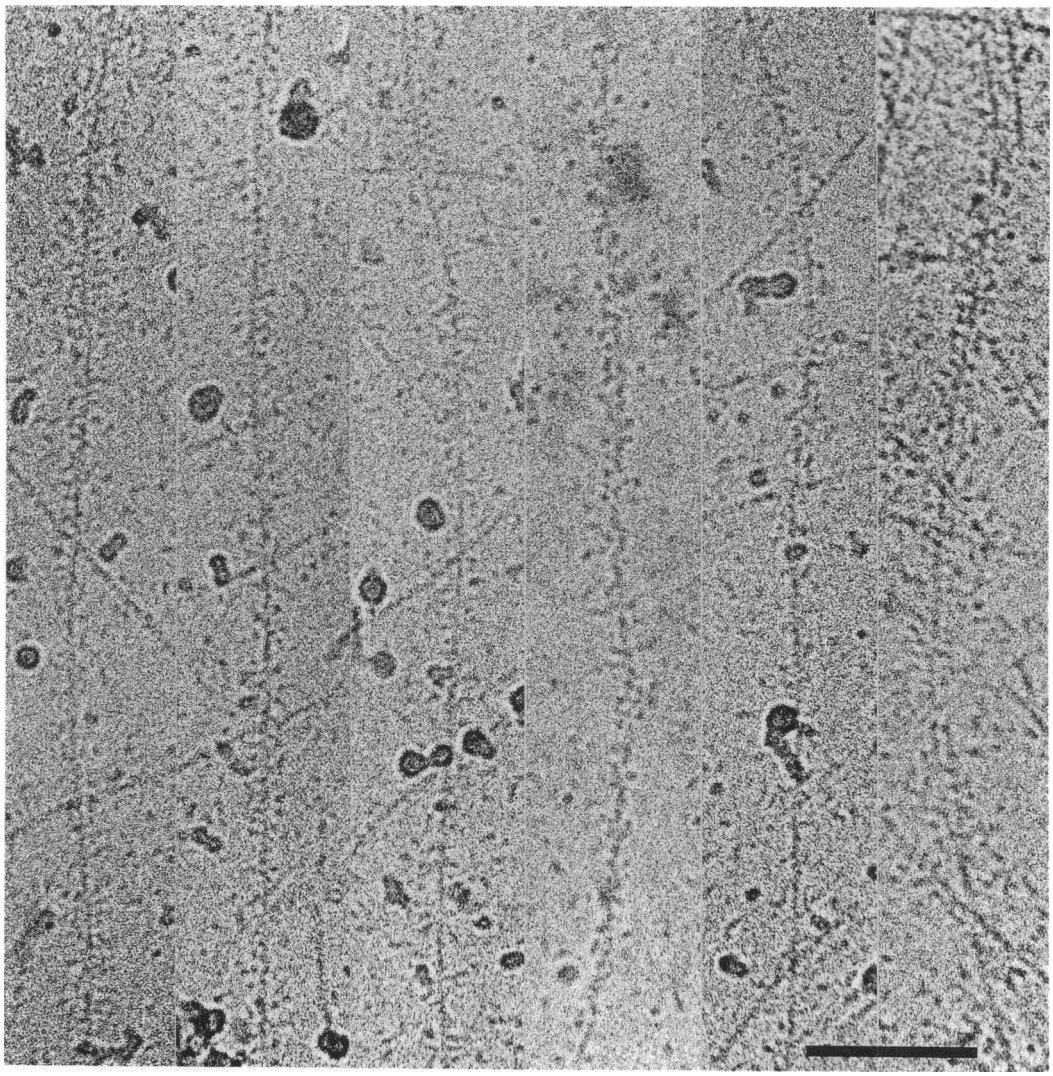

FIGURE 4 Montage of filament decorated with cardiac muscle S1 in steady-state ATP hydrolysis. Note the appearance of lines of S1 slightly separated from the actin filament by a region of low density; this is best seen by sighting down the filament from the edge of the micrograph. The scale bar shows 100 nm.

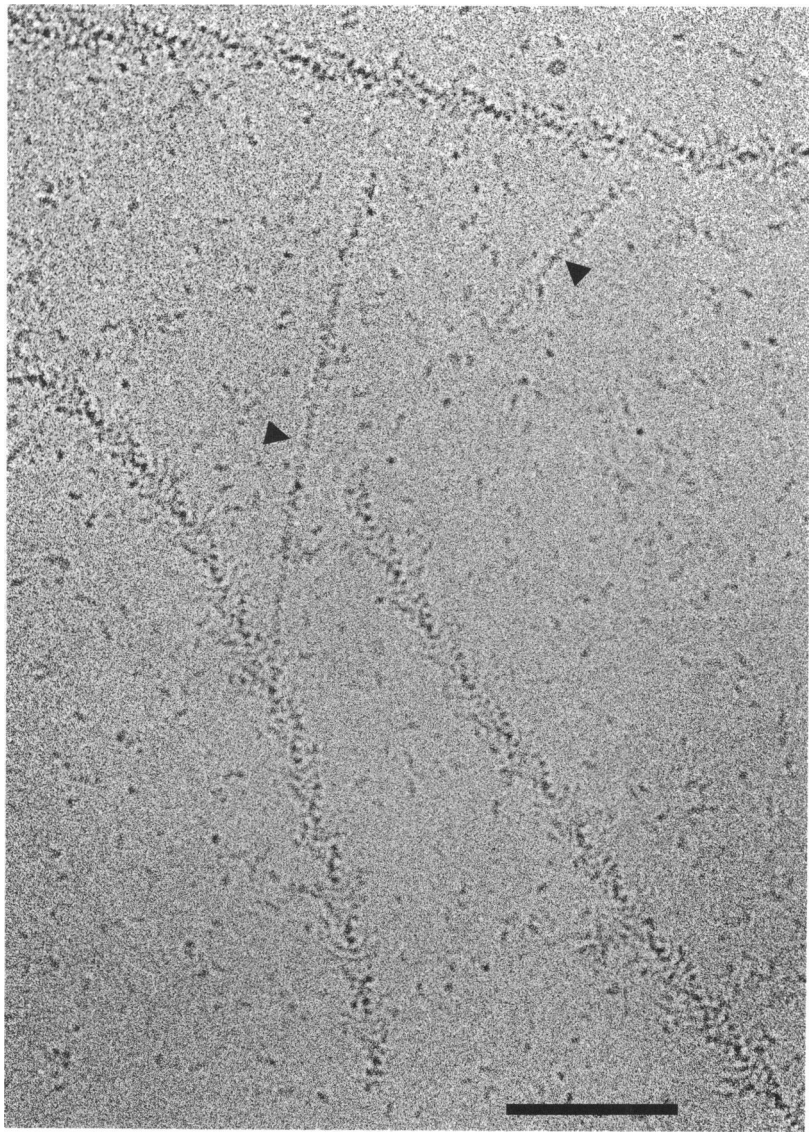

FIGURE 5 Actin in the presence of cardiac muscle S1 after exhaustion of ATP. Note the decorated and undecorated filaments (*single arrows* mark undecorated filaments). The scale bar shows 100 nm.

of S1 at the so-called rigor angle of roughly 45° to the filament long axis (Huxley, 1963; Milligan and Flicker, 1987; Moore et al., 1970). An unexpected feature of such specimens was that when the molar concentration of the S1 was less than that of actin, the actin filaments were not all decorated to the same extent. Instead, some of the filaments appeared fully decorated whereas others appeared completely unlabelled. This apparently cooperative behavior of S1 attachment in ADP is probably not the result of heterogeneity in the actin or S1, because when the S1 was stoichiometric with the actin full decoration was observed. The change from partial decoration in ATP to either full or no decoration in ADP is consistent with the S1 dissociating and reassociating in ATP. Rigor binding of the S1 was not however completely cooperative, because at low ratios of S1 examples of what seem to be partial labelling could also be found. (The ratio of S1 to actin used varied between 1:1 and 1:10). Examples of this are seen in Fig. 6. Where the labelling was partial the S1 was also attached at an angle of approximately 45°.

DISCUSSION

Some form of tilting-bridge mechanism remains the most likely origin of muscle force. Although this hypothesis was first put forward more than 2 decades ago, firm evidence of more than one attached geometry of the myosin head has proven very elusive. One of the main impediments to progress has been the instability of the acto-S1 complex in the presence of ATP under conditions compatible with electron microscopy methods for solutions. Two approaches mainly have been used to overcome this: cross-linking and low ionic strength. Although microscopy of cross-linked acto-S1 complex has clearly shown a variety of attached configurations (Craig et al., 1985; Applegate and Flicker, 1987), it cannot be ruled out that this behavior results merely from the cross-link acting as a hinge.

The present experiments relied on the use of very low ionic strength (~2 mM) to promote association of the acto-S1-ATP complex. Light-scattering experiments carried out in

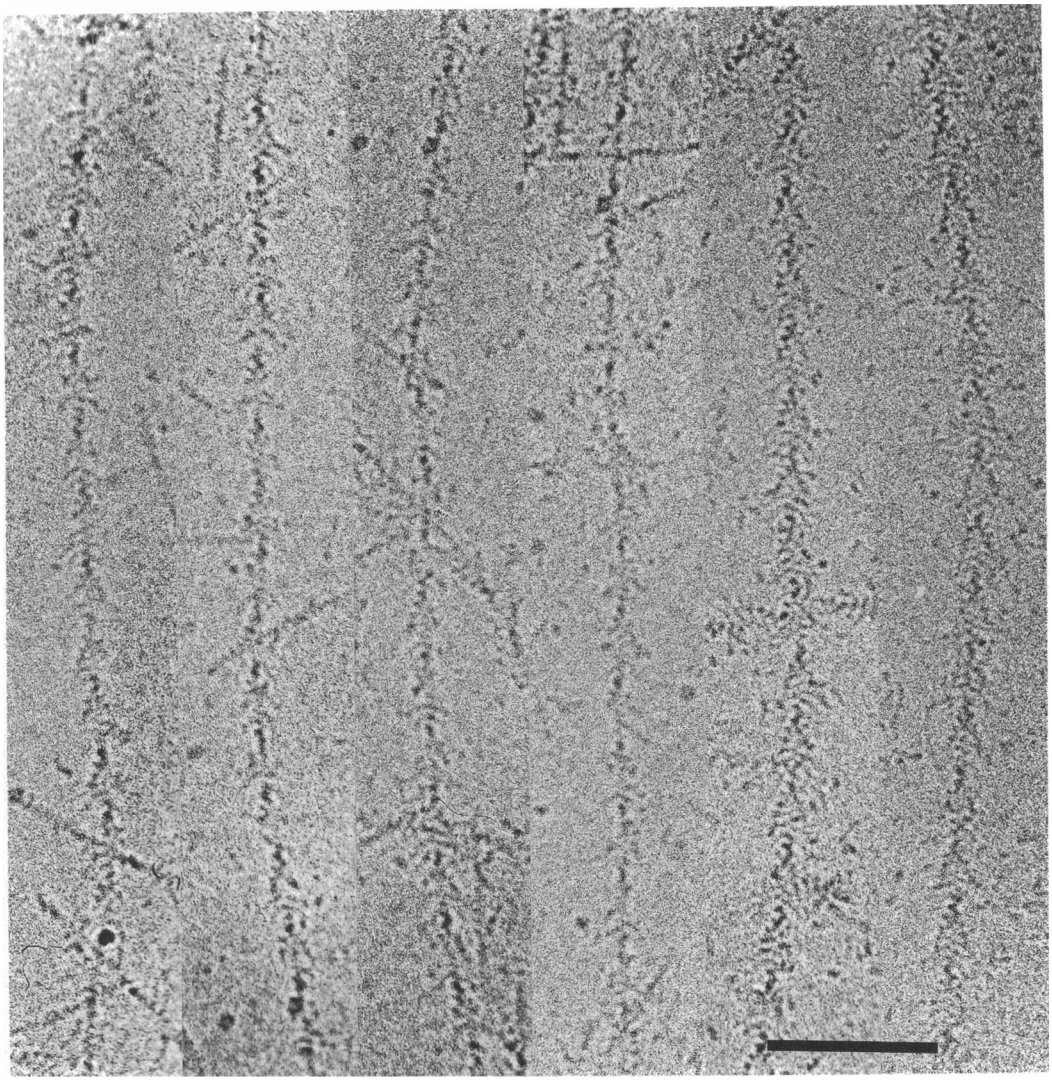

FIGURE 6 Montage of filaments decorated with cardiac S1 after exhaustion of ATP. The first four panels (from the left) show partial labelling; the last two appear fully labelled. The scale bar shows 100 nm.

parallel with the electron microscopy indicate that approximately 70% of the S1 can be attached to actin during steady-state hydrolysis, and the micrographs obtained are compatible with this estimate. The effect of lowering the ionic strength from physiological to 2 mM is primarily to increase the on-rate of binding of the S1-nucleotide complex to actin by approximately 1000-fold, whereas the off-rate is essentially independent of ionic strength (White and Taylor, 1976). It could be argued that such a low ionic strength might result in structural changes that are not representative of the normal cross-bridge cycle. For instance, binding of the LC1 myosin light chain to actin has been demonstrated (Trayer et al., 1987), and it is conceivable that the attachment of S1 in the presence of ATP seen here might be the result of this interaction. However, the fact that the ATPase rate increases monotonically as the salt concentration is lowered (White and Taylor, 1976) argues that the predominant effect of low ionic strength is to increase the affinity of the same intermediates that are weakly bound in higher salt. This suggests there is no new type of interaction in low salt. Similarly, binding of both A1-S1 and A2-S1 increase progressively as ionic strength is reduced (Chalovitch et al., 1984), which also suggests that the mode of attachment in low salt is not fundamentally different from that at higher ionic strength.

The micrographs of specimens frozen during steady-state ATP hydrolysis show disordered binding of the S1 to actin. This indicates more than one S1 attachment geometry. In many cases individually bound S1 molecules can be seen in configurations different from the well characterized rigor conformation. These conclusions are in accord with earlier studies (Craig et al., 1985; Applegate and Flicker, 1987; Frado and Craig, 1992); however, the use of unstained hydrated specimens should be less subject to artifacts than other electron microscopy methods, and cross-linking was not used. Because the binding sites for S1 on the actin filament are approximately helically arranged, individual attachment angles cannot be directly measured from a single image. However, the fact that S1 molecules can be found at angles

<90° and >90° on the same filament also indicates that the attachment configuration is variable. We cannot rule out that some of the S1 has recently detached and is lying alongside the filament, but the incidence of this is probably low, because S1 will rapidly diffuse away once detached.

In some of the clearest cases where individually attached S1 molecules could be discerned, the attachment angle made with the filament was approximately 90°, which is similar to behavior reported by Frado and Craig (1992). The micrographs are not sufficiently detailed to decide whether the different attachment geometries result from a change in angle of attachment with actin or from a conformational change within the S1 itself. It is also difficult to explain the appearance seen in many decorated filaments in ATP of a region of low density near the filament and a row of higher density at higher radius, because the bulkiest part of S1 is near the actin binding site (Milligan and Flicker, 1987). One possible reason for this behavior is that there was a gross change in the shape of the S1, such that the distal part of the molecule is turned to run roughly parallel to the filament axis. This appearance is probably not due to an underfocus fringe, because similar behavior can be seen closer to focus although with less contrast.

Although the rate of dissociation and reassociation of S1 is rapid compared with the other steps in the ATP hydrolysis mechanism ($\sim 10^3$ s^{-1} under the conditions in Figs. 1–4) it is approximately 100 times slower than the time required to vitrify the specimen ($\sim 10^5$ s-1, Mayer and Astl, 1992). The freezing rate is therefore sufficiently rapid to trap these intermediates in the state in which they exist just before freezing. There is however considerable evidence from electron paramagnetic probe studies of actomyosin that there are large scale motions of myosin heads bound to actin during ATP hydrolysis, on a time scale of $\sim 10^6$ s^{-1} (Berger and Thomas, 1989; Berger and Thomas, 1993). Motions occurring on a time scale comparable or more rapid than the freezing could account for some of the observed variability of S1 attachment.

The present experiments lead to different conclusions from the recent work by Pollard et al. (1993) who also described the acto-S1 complex at low ionic strength during steady-state hydrolysis (see also Funatsu et al., 1993). Their study, which was based on metal-shadowed replicas of the complex after freeze-fracture and deep etching, did not reveal any differences in attached S1 configuration from the rigor state. It is not clear why the appearance of the complex should be different when prepared by these different methods. As well as the differences in procedure after freezing, the deep-etched specimens also included 10% methanol to retard ice crystal formation. To confirm that this had no effect, we included methanol in some of the hydrated specimens frozen during ATP hydrolysis. Preliminary data from these showed disordered heads and appeared similar to controls without methanol. In a separate study using deep-etching it was reported that heads are shorter in ATP (Katayama, 1989).

In control experiments after exhaustion of the ATP the S1 tended to bind to actin cooperatively in ADP. Thus with substoichiometric amounts of S1 a mixture of completely (or heavily) labelled filaments and unlabelled filaments was obtained, although what appeared to be partial decoration was also seen. We were unable to produce more even labelling by mixing actin and S1 together in the absence of a nucleotide in a simple rapid mixing device (data not shown). Cooperativity could indicate that the actin filament is switched on in some way when S1 is first bound. Alternatively there may be some interaction between the S1-bound molecules. A tendency toward cooperative decoration was also observed previously in negatively stained specimens (Craig et al., 1980).

The quite different images of filaments decorated in ATP from those in ADP are compatible with tilting-bridge models of force generation, but they do not, of course, provide proof. Stronger evidence will come if it can be shown that different kinetic states in the ATPase cycle are associated with substantially different attached S1 geometries. Experiments on presteady-state kinetics indicate that the primary bound intermediate during steady-state ATP hydrolysis under the conditions used here is A-M-ATP (Belknap et al., 1993). It will, therefore, be important to examine the structure of the other weakly attached state M.ADP.Pi, especially as calculations of the free energy changes at different stages in the ATPase cycle suggest that product release is likely to be associated with force generation (White and Taylor, 1976).

We thank I. Rayment and R. Smith for providing the method for making cardiac S1 and P. Knight and G. Offer for comments on the manuscript. This work was supported by grants from the American Heart Association, the Agricultural and Food Research Council (United Kingdom) and NIH grant HL41776 issued to HW.

REFERENCES

Adrian, M., J. Dubochet, J. Lepault, and A. McDowall. 1984. Cryo-electron microscopy of viruses. *Nature (Lond.)*. 308:32–36.

Applegate, D., and P. Flicker. 1987. New states of acto-myosin. *J. Biol. Chem.* 262:6856–6863.

Belknap, B., X. Q. Wang, and H. White. 1992. The bond splitting step is rate limiting for skeletal actomyosin S1 ATP hydrolysis. *Biophys. J.* 61: 440a.

Berger, C. L., and D. D. Thomas. 1989. Photolysis of a photolabile precursor of ATP (caged ATP) induces microsecond rotational motions of myosin heads bound to actin. *Proc. Natl. Acad. Sci. USA*. 86:8753–8757.

Berger, C. L., and D. D. Thomas. 1993. Rotational dynamics of actin-bound heads in active myofibrils. *Biochemistry*. 32:3812–3821.

Chalovitch, J. M., L. A. Stein, L. E. Greene, and E. Eisenberg. 1984. Interaction of isozymes of myosin subfragment-1 with actin - effect of ionic strength and nucleotide. *Biochemistry*. 23:4885–4889.

Craig, R., L. Alamo, and R. Padron. 1992. Structure of the Myosin Filaments of Relaxed and Rigor Vertebrate Striated Muscle Studied by Rapid Freezing Electron Microscopy. *J. Mol. Biol.* 228:474–487.

Craig, R., L. E. Greene, and E. Eisenberg. 1985. Structure of the Actin Myosin Complex in the Presence of ATP. *Proc. Natl. Acad. Sci. USA*. 82:3247–3251.

Craig, R., A. G. Szent-Gyorgyi, L. Beese, P. Flicker, P. Vibert, and C. Cohen. 1980. Electron microscopy of thin filaments decorated with Ca^{2+}-regulated myosin. *J. Mol. Biol.* 140:35–55.

Danzig, J. W., Y. E. Goldman, N. C. Millar, J. W. Lacktis, and E. Homsher. 1992. Reversal of cross-bridge force generating transition by photogeneration of phosphate in rabbit psoas muscle fibres. *J. Physiol. (Lond.)*. 451:247–278.

Flicker, P., T. Wallimann, and P. Vibert. 1983. Electron microscopy of scallop myosin: location of the regulatory light chain. *J. Mol. Biol.* 169: 723–741.

Frado, L. L., and R. Craig. 1992. Electron microscopy of the actin-myosin head complex in the presence of ATP. *J. Mol. Biol.* 223:391–397.

Funatsu, T., E. Kono, and S. Tsukita. 1993. Time-resolved electron-microscopic analysis of the behaviour of myosin heads on actin filaments after photolysis of caged ATP. *J. Cell Biol.* 121:1053–1064.

Hibberd, M. G., and D. R. Trentham. 1986. Relationship between chemical and mechanical events during muscle contraction. *Ann. Rev. Biophys. Biophys. Chem.* 15:119–161.

Hirose, K., T. D. Lenart, J. M. Murray, C. Franzini-Armstrong, and Y. E. Goldman. 1993. Flash and smash: rapid freezing of muscle fibres activated by photolysis of caged ATP. *Biophys. J.* 65:397–408.

Huxley, H. E. 1963. Electron microscope studies of natural and synthetic protein filaments from striated muscle. *J. Mol. Biol.* 7:281–308.

Huxley, H. E. 1969. The mechanism of muscle contraction. *Science (Wash. DC).* 164:1356–1366.

Katayama, E. 1989. The effects of various nucleotides on the structure of actin-attached myosin subfragment-1 studied by quick freeze deep-etch electron microscopy. *J. Biochem.* 106:751–770.

Mayer, E., and G. Astl. 1992. Limits of cryofixation as seen by Fourier transform infrared spectroscopy of metmyoglobin azide and carbonyl hemoglobin in vitrified and freeze-concentrated aqueous solution. *Ultramicroscopy.* 45:185–197.

Milligan, R. A., and P. F. Flicker. 1987. Structural relationships of actin, myosin, and tropomyosin revealed by cryo-electron microscopy. *J. Cell Biol.* 105:29–39.

Moore, P. B., H. E. Huxley, and D. J. DeRosier. 1970. Three-dimensional reconstruction of F-actin, thin filaments and decorated thin filaments. *J. Mol. Biol.* 50:279–295.

Pollard, T. D., D. Bhandari, P. Maupin, D. Wachsstock, A. G. Weeds, and H. G. Zot. 1993. Direct visualization by electron-microscopy of the weakly bound intermediates in the actomyosin adenosine-triphosphatase cycle. *Biophys. J.* 64:454–471.

Rayment, I., W. R. Rypniewski, K. Schmidtbase, R. Smith, D. R. Tomchick, M. M. Benning, D. A. Winkelmann, G. Wesenberg, and H. M. Holden. 1993. 3-dimensional structure of myosin subfragment-1 - a molecular motor. *Science (Wash. DC).* 261:50–58.

Stein, L. A., L. E. Greene, P. B. Chock, and E. Eisenberg. 1985. Rate-limiting step in the actomyosin adenosine-triphosphatase cycle - studies with myosin subfragment-1 cross-linked to actin. *Biochemistry.* 24:1357–1363.

Trayer, I. P., H. R. Trayer, and B. A. Levine. 1987. Evidence that the N-terminal region of A1 light chain of myosin interacts directly with the C-terminal region of actin. *Eur. J. Biochem.* 164:259–266.

Trinick, J., and J. Cooper. 1990. Concentration of solutes during preparation of aqueous suspensions for cryo-electron microscopy. *J. Microsc. (Oxf.).* 159:215–222.

Trinick, J., J. Cooper, J. Seymour, and E. H. Egelman. 1986. Cryo-Electron Microscopy and 3-Dimensional Reconstruction of Actin-Filaments. *J. Microsc. (Oxf.).* 141:349–360.

Tsukita, S., and M. Yano. 1985. Actomyosin Structure In Contracting Muscle Detected By Rapid Freezing. *Nature (Lond.).* 317:182–184.

Vale, R. D., and F. Oosawa. 1990. Protein motors and Maxwell's demons: does mechanochemical transduction involve a thermal ratchet? *Adv. Biophys.* 26:97–134.

Vibert, P., and R. Craig. 1982. Three-dimensional reconstruction of thin filaments decorated with a Ca^{2+}-regulated myosin. *J. Mol. Biol.* 157: 299–319.

Walker, M., and J. Trinick. 1989. Electron-microscopy of negatively stained scallop myosin molecules - effect of regulatory light chain removal on head structure. *J. Mol. Biol.* 208:469–475.

Weeds, A. G., and R. S. Taylor. 1975. Separation of subfragment 1 isoenzymes from rabbit skeletal muscle myosin. *Nature (Lond.).* 257:54–56.

White, H. D., and E. W. Taylor. 1976. Energetics and mechanism of actomyosin adenosine triphosphatase. *Biochemistry.* 15:5818–5825.